

JGP 100th Anniversary

A perspective on Na and K channel inactivation

Clay M. Armstrong and Stephen Hollingworth

Department of Physiology, University of Pennsylvania, Philadelphia, PA

We are wired with conducting cables called axons that rapidly transmit electrical signals (e.g., "Ouch!") from, for example, the toe to the spinal cord. Because of the high internal resistance of axons (salt water rather than copper), a signal must be reinforced after traveling a short distance. Reinforcement is accomplished by ion channels, Na channels for detecting the signal and reinforcing it by driving it further positive (to near 50 mV) and K channels for then restoring it to the resting level (near -70 mV). The signal is called an action potential and has a duration of roughly a millisecond. The return of membrane voltage (V_m) to the resting level after an action potential is facilitated by "inactivation" of the Na channels: i.e., an internal particle diffuses into the mouth of any open Na channel and temporarily blocks it. Some types of K channels also show inactivation after being open for a time. N-type inactivation of K channels has a relatively fast time course and involves diffusion of the N-terminal of one of the channel's four identical subunits into the channel's inner mouth, if it is open. This mechanism is similar to Na channel inactivation. Both Na and K channels also display slower inactivation processes. C inactivation in K channels involves changes in the channel's outer mouth, the "selectivity filter," whose normal function is to prevent Na^+ ions from entering the K channel. C inactivation deforms the filter so that neither K^+ nor Na^+ can pass.

In 1952, Hodgkin and Huxley made a giant step in understanding the nerve impulse. They explained the action potential as the result of a rise of Na^+ permeability, which forces membrane voltage (V_m) to be positive, followed by "inactivation" of Na^+ permeability and a rise of K^+ permeability to restore V_m to the resting level (Hodgkin and Huxley, 1952a,b,c). At the time, the means of ion transport across the membrane, whether ion carrier, ion channel, or simply diffusion of ions through the bilipid layer, was unknown. Hodgkin and Huxley leaned toward, but ultimately rejected, the idea of ion carriers, which seemed to provide a simpler mechanism for ion selectivity; and they used the electrical terms g_{Na} and g_K instead of permeability (Hodgkin and Huxley, 1952a,b). Using "voltage clamp" experiments on squid axons, they found that g_K had the simpler kinetics, a sigmoid increase after a positive (depolarizing) step of membrane potential and an exponential decline upon repolarization. To explain these kinetics, Hodgkin and Huxley (1952d) postulated that g_K was controlled by four positively charged "n particles," which moved outward, independently, through the membrane field to activate the conductance (or four negative n particles moving inward). Each particle reached its activating site with exponential kinetics, for which the rate constants were voltage dependent. Activation required that all four particles be in place, and g_K was thus proportional to n^4 . (Legend has it that Huxley invented this scheme, which provides a sigmoid rise of conductance and an exponential decline. They noted that n^6 would provide a better fit, but was too much trouble with a hand calculator.) Similarly, activation kinetics of the Na^+ conductance were explained



by three m particles, but another particle called h moved more slowly to "inactivate" the conductance. Overall,

$$g_K = n^4 \times \bar{g}_K$$

and

$$g_{\text{Na}} = m^3 h \times \bar{g}_{\text{Na}},$$

where \bar{g}_K and \bar{g}_{Na} are the maximum conductances. The variable m increases rapidly from 0 to 1, with strong depolarization, whereas h declines more slowly from 1 to 0. The variable n increases relatively slowly, from 0 to a maximum of 1.

The physical basis for these events was unclear for many years. Some of the earliest evidence for the existence of a transmembrane channel was from experiments that examined block of K channels by an internally applied TEA^+ ion, a cation about the same size as a hydrated K^+ ion. When added to the internal medium, TEA^+ appeared to enter the "channel" through an internal "gate" after a positive step of V_m opened the gate, and to occupy a "vestibule." TEA^+ motion outward through the channel was arrested by a narrow zone, the selectivity filter (SF), a felicitous name invented by Bertil Hille (1971, 1975) for the Na channel. K^+ ions dehydrated to pass through the filter, but TEA^+ , with its covalently attached ethyl groups, could not pass, and the open channel became blocked. TEA^+ cleared out of the channel on repolarization. Its exit

Correspondence to Clay M. Armstrong: carmstro@mail.med.upenn.edu

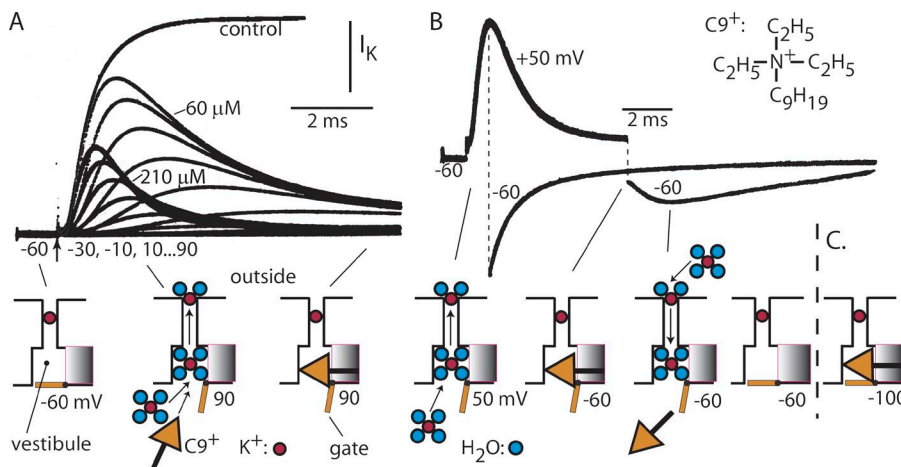


Figure 1. C9^+ block of I_K resembles inactivation of I_{Na} . (A) I_K (in squid axon) increases sigmoidally to a constant level after a depolarization to 90 mV (trace labeled control). With 60 μM C9^+ inside the axon, I_K increases normally and then “inactivates” (steps to $-30 \dots 90$ mV). C9^+ enters more rapidly with 210 μM inside, resulting in smaller peak current and faster inactivation. The diagram shows the interpretation. At rest (-60 mV), a gate at the inner end of the channel protects a vestibule wide enough to hold a hydrated K^+ ion, ~ 8 Å in diameter. When the gate is opened by depolarization, K^+ ions enter the vestibule, dehydrate as they pass through a narrow SF, and rehydrate at the outer end of the filter. C9^+ , also about ~ 8 Å in

diameter but with a nonyl tail, enters the vestibule much more slowly than K^+ , at a rate proportional to its concentration. Because its ethyl arms are covalently linked, it cannot shed them to enter the SF. Its hydrophobic nonyl chain binds to a hydrophobic region in the vestibule wall. Inactivation is faster at the higher C9^+ concentration. (B) C9^+ is forced out of the vestibule on repolarization to -60 mV by an influx of K^+ ions. At the end of a short pulse, which results in a block of a few channels, I_K is inward (external $[\text{K}^+]$ is high) and initially large, but decays rapidly as the channels deactivate. After a longer pulse, which inactivates most channels, I_K is initially small, but increases as C9^+ is driven from the vestibule by the in-moving K^+ . A channel liberated of C9^+ can then close. (C) If V_m is returned to -100 , the gate is slammed shut, trapping C9^+ in the vestibule. In that case, the next depolarization, 2 s later, results in no I_K : the channels are still C9^+ blocked (not depicted). (Modified from Armstrong, 2007).

was hastened by high external K^+ , which swept TEA^+ from the channel's inner vestibule (or cavity) and gate region, so that the gate at the cytoplasmic end of the channel could then close.

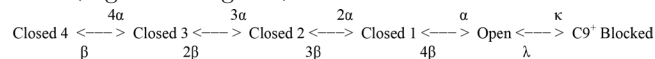
Squid K channel “inactivation” with C9^+

Squid axons with “ C9^+ ” (nonyl-triethylammonium ion) rather than TEA^+ inside showed “inactivation” of I_K : a relatively slow decline of I_K qualitatively similar to the inactivation normally seen with Na channels. Because of its nine-carbon tail, C9^+ has a much higher affinity for the inner vestibule of the channel than does TEA^+ . It is now known that the vestibule and the gating region at the inner end of the channel have hydrophobic walls formed by the side chains of hydrophobic residues, e.g., leucine, isoleucine, valine, and phenylalanine. The hydrophobic tail of C9^+ binds to these walls, making it possible to block with low C9^+ concentrations. C9^+ can enter a K channel only when the activation gate at the inner end of the channel has been opened by depolarization. When present in the axoplasm at low concentration, C9^+ diffuses slowly into the open channel and blocks it.

The result, as shown in Fig. 1, is a slow decline of current during a depolarizing pulse, which is similar to the inactivation that occurs in a Na channel. If C9^+ blocks all of the channels, there is no current immediately on repolarization, but, with K^+ outside, a slowly growing and then decaying inward tail current of K^+ is seen as C9^+ clears out of the channels, moving to the axoplasmic side. The slow decline of this current shows that C9^+ in a channel not only blocks I_K but also prevents the channel gates from closing (Fig. 1). Inward I_K , through the still-open channel

gate, grows in magnitude for some milliseconds after the end of the voltage clamp pulse, when C9^+ clears out of the channels, causing a “hook in the tail.” The current then declines as the voltage-dependent gates are forced closed, as we now know, by the downward motion of the S4 segments, responding to negative V_m .

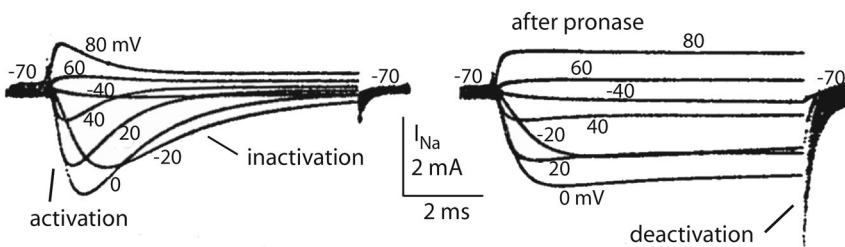
Inactivation caused by C9^+ in the K channel and its recovery on repolarization can be well reproduced by the following kinetic scheme (Scheme 1; Fitzhugh, 1965; Armstrong, 1969). Scheme 1 has a significant difference from the m^3h formulation of Hodgkin and Huxley, in which the variables m and h are independent of each other, making it possible for inactivation to be complete ($h = 0$) while the channels are completely closed ($m = 0$). With the C9^+ kinetic scheme, in contrast, C9^+ block can be achieved only if the channel is in the open state. Further, the channel gate cannot close (at -60 mV) if C9^+ is in the channel. As shown in Fig. 1 B, when V_m is returned to -60 mV, I_K is initially very small, but grows as C9^+ exits the channels, which are then free to close. At -100 mV, the gate closes and traps C9^+ in the vestibule (Fig. 1 C, diagram).



(Scheme 1)

Na channel inactivation

A next step in the study of inactivation, this time in the Na channel, was the discovery that pronase, a nonspecific protease used to facilitate internal perfusion of



and upon repolarization, there is a large inward current through the still active channels. Each trace in the figure was for a depolarization from -70 mV to the indicated voltage, with a 2-s interval between depolarizations. I_{Na} is outward at 60 and 80 mV, where the voltage drives Na^+ outward through the channels. (Modified from Armstrong et al., 1973.)

squid axons (Armstrong et al., 1973), removed inactivation (Fig. 2). This led to the “ball and chain” model of Na inactivation. The idea is that a “ball,” analogous to $C9^+$, is attached to the inner part of the Na channel, and pronase snips the chain that secures the inactivation ball in position (Armstrong and Bezanilla, 1977; Bezanilla and Armstrong, 1977). At the time, even the existence of a Na channel protein was uncertain, and the pronase effect suggested that, at least part of the channel (also a disputed word), was protein.

From the left trace in Fig. 2 it can be seen that the normal channel with intact inactivation does not “leak” after repolarization: there is a very brief tail of current as the channels that have not inactivated close but nothing like the large, rapidly decaying tail seen after pronase (Fig. 2, right), or the prolonged tail of I_K seen in Fig. 1 C as $C9^+$ leaves the $C9^+$ -blocked channels. In the kinetic scheme above (Scheme 1), the I_K tail is produced by the reflux of the channels through the open state as $C9^+$ exits. Clearly, for the inactivated Na channel, there must be a way to bypass the conducting state during recovery from inactivation. A scheme for accomplishing this bypass is given in Fig. 7. (A somewhat similar scheme was presented in the original paper [Armstrong, 1971].)

The recording of gating current (I_g ; Armstrong and Bezanilla, 1973) provided another element to the study of inactivation. I_g was initially predicted by Hodgkin and Huxley and was postulated to arise from the movement of charged m , h , and n particles that control g_{Na} and g_K . It is now known that I_g is produced by the movement of positive charges in the S4 segments of the Na and K channel proteins, as described below. Fig. 3 shows inward I_{Na} recorded from a squid giant axon. After adding tetrodotoxin to block the Na channels, an outward I_g can be seen, $\sim 10\times$ smaller than I_{Na} in the conditions used (reduced $[Na^+]_{out}$). I_g has a component with a fast rise and fall, temporally associated with the rise of I_{Na} . This is followed by a small, slow component (Fig. 3, arrow). It was too slow to be associated with activation and too fast to be directly associated with the inactivation seen in the I_{Na} trace. Further, it was unaf-

affected when pronase was used to destroy inactivation. The function of this slow component was not identified clearly at the time of the experiment, but it seemed to prepare the channels for inactivation. It is discussed below, in connection with Fig. 7.

The experiments further showed that, after a pulse too short for appreciable inactivation to occur, all of the gating charges returned quickly to rest, but with a pulse long enough for inactivation to reach a steady-state, $\sim 60\%$ of the gating charge was temporarily “immobilized” (Fig. 4; Armstrong and Bezanilla, 1977). It returned to the resting position with the relatively slow time course of recovery from inactivation (not depicted). Removal of inactivation with pronase, known since Stühmer et al. (1989) to cut the linker between domains 3 and 4, completely removed charge immobilization (Armstrong and Bezanilla, 1977).

During the 1980s, there were great accomplishments in the study of Na and K channels. Na channel protein was isolated (Agnew et al., 1980) and subsequently sequenced by the laboratory of Shosaku Numa (Noda et al., 1984). In the original drawings of Noda et al. (1984), the S4 sequences were shown to be internal, rather than transmembrane. Apocryphally, one of us was told the S4s returned to the membrane after Numa read a 1981 review that contained a sliding “zipper” model (Armstrong, 1981). The Shaker K channel was cloned and sequenced in 1987 (Baumann et al., 1987; Kamb et al., 1987; Papazian et al., 1987; Tempel et al., 1987). Cloning of Na and K channels, coupled with the development of the patch clamp techniques (Neher and Sakmann, 1976; Neher et al., 1978; Hamill et al., 1981), opened the doors to a molecular and physiological understanding of channel function. The vast literature subsequently generated by many thoughtful and creative scientists is beyond the scope of this review. A significant fraction of this literature was published in *Journal of General Physiology*, a testimony to the editors and to the high standard of reviewing sustained by the journal. Here, with apologies, we mention only some results from this era, before focusing on a more-recent structural understanding of inactivation.

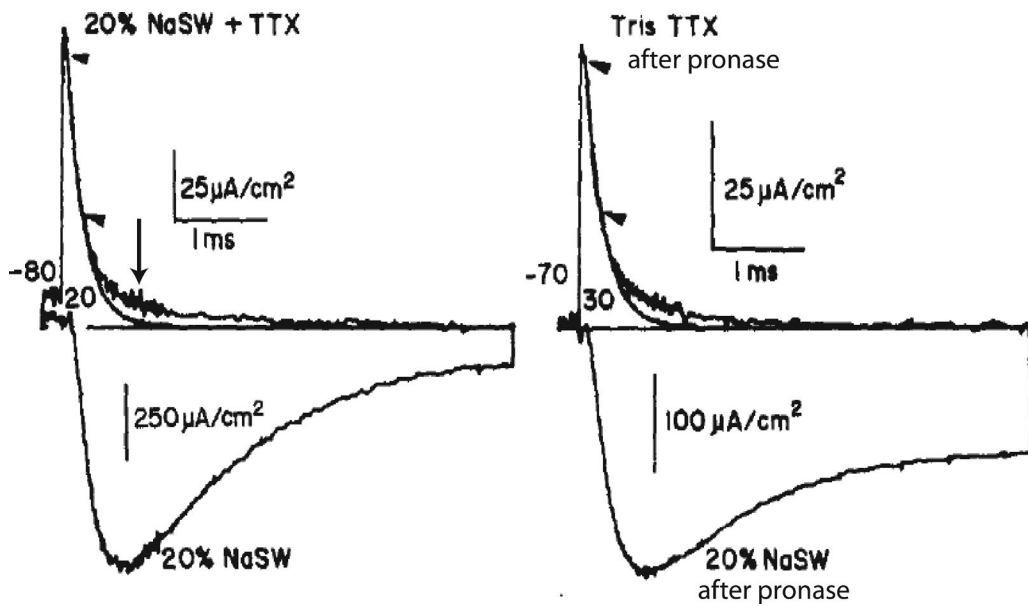


Figure 3. I_g and I_{Na} . I_g is generated by the voltage-driven movement within the membrane of charged "particles," now known to be arginine and lysine residues on the S4 helices. This movement forces the conformational changes that open and close the activation gate. In the traces shown, I_K was eliminated by removing all K^+ inside and out, and I_{Na} was reduced by lowering $[Na^+]$ (lower traces), or completely suppressed by adding tetrodotoxin. Capacitive current was removed by subtraction. (Left) For a step to 20 mV, I_g is outward and decays rapidly after its peak. The smooth trace is a fitted exponential to this fast phase of decay. A much smaller, slow component follows (arrow). It is too fast to be directly associated with inactivation of I_{Na} , but in Fig. 6 is related to a step preparatory to inactivation. (Right) After most of inactivation has been removed by pronase, the slow component is unchanged, further evidence that it is not directly related to inactivation.

An important early result came from patch-clamp measurements of single- Na channels (Aldrich et al., 1983) and Shaker K channels (Zagotta and Aldrich, 1990). With both channel types, closing to the inactivated state is not strongly voltage-dependent, consistent with the ball and chain model, which assumes the inactivating particle is not only uncharged but also does not enter the electric field. Further, with small, depolarizing steps, τ_h (the inactivation time constant in a Hodgkin-Huxley analysis), best fits not inactivation, but the late time course of activation (Aldrich et al., 1983), again consistent with the ball and chain model.

The first molecular understanding of the ball and chain idea came from the intact Shaker K channel, which was found to inactivate through open channel block by a built-in inactivation "ball" at the N terminus of each of its four subunits, giving rise to the term "N-type inactivation" (Hoshi et al., 1990; Zagotta et al., 1990). By using Shaker K channel constructs with zero to four N-terminals, they found that inactivation rate was proportional to the number of intact terminals in the construct and did not occur if there were none: inactivation occurred when any one of the N-terminals enters the channel's inner mouth, much in the manner of $C9^+$. Inactivation

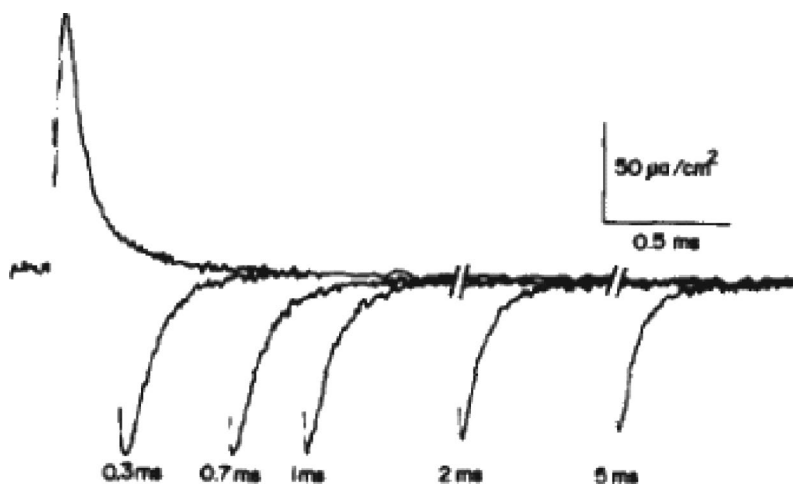


Figure 4. **Immobilization of gating charge by inactivation.** I_g is shown for an axon with no Na^+ or K^+ either in or out, elicited by a step from -70 mV to 20 mV, with return to -70 mV after the interval indicated. The inward tail of I_g on repolarization decreases with time as the Na channels inactivate, immobilized by inactivation. Approximately 60% of total charge movement is immobilized by a long pulse.

with four N-terminals is faster, analogous to raising the C9^+ concentration. As with C9^+ , closing of the channel gate occurs after the N-terminal dissociates from the channel's gate region. Gating current measurements show that the four S4 domains of the Shaker K channel are immobilized as long as the channel gate is held open (Perozo et al., 1992; Stefani et al., 1994). Turning to the Na channel, the ball and chain are now identified with the linker between domains 3 and 4 (Vassilev et al., 1988; Stühmer et al., 1989), making it clear that the ball is attached by a chain on both sides, rather than by a single chain. This general idea is sometimes referred to as a "hinged lid" (West et al., 1992).

Hoshi et al. (1991) described a much slower type of K-channel inactivation, which they called C type (or C inactivation), very distinct from N type. C inactivation is conceptually useful in explaining phenomena slower than the action potential, e.g., short-term memory. It is associated with the outer carbonyl ring of the SF, which is crucial for binding dehydrated K^+ ions. A possible sequence of events triggering C inactivation was outlined by Hoshi and Armstrong (2013), based on the K-channel structure of Long et al. (2007). The carbonyl oxygens in the SF mimic the inner hydration shell of a K^+ ion, and their precise location is essential for the channel to select and conduct K^+ ions (Doyle et al., 1998; Zhou et al., 2001). Fig. 5 A shows the carbonyl oxygens of Y373 (Y445 in Shaker), one from each of the four subunits in the Long et al. (2007) K channel structure. They form part of the outermost K^+ binding site in the SF. Each of the Y373 (Sh Y445) residues is stabilized in position by interaction with surrounding residues, particularly with W362 (Sh W434) and V377 (Sh T449) (Fig. 5 A). Mutation of the equivalent residues in the Shaker K channel profoundly alters C inactivation. W434F is permanently C-type inactivated without disturbing S4 motion in response to a voltage change, making W434F channels very valuable in the study of K channel I_g (Perozo et al., 1993). Mutation of V377 (Sh T449) to alanine speeds C inactivation.

How are these residues affected by activation of the channel? In one proposal (Fig. 5 B), depolarization drives the S4 segment outward, bringing S4 residue R293 (Sh R365) into contact with F344 (Sh F416) in S5 of a neighboring subunit (Hoshi and Armstrong, 2013). This contact initiates a conformational wave that spreads from F344 (Sh F416) to residues near the SF, where the wave breaks a hydrogen bond between D375 (Sh D447) and W362 (Sh W434). This destabilizes W362 (Sh W434) and permits Y373 (Sh Y445) to rotate so that its carbonyl oxygen moves away from the pore axis. As a result, binding affinity of the outer ring drops drastically, lowering K^+ occupancy. In the absence of a bound K^+ , the carbonyls of the ring repel each other, causing the ring to further expand and erasing its ability to bind dehydrated K^+ ions; the channel is "inactivated."

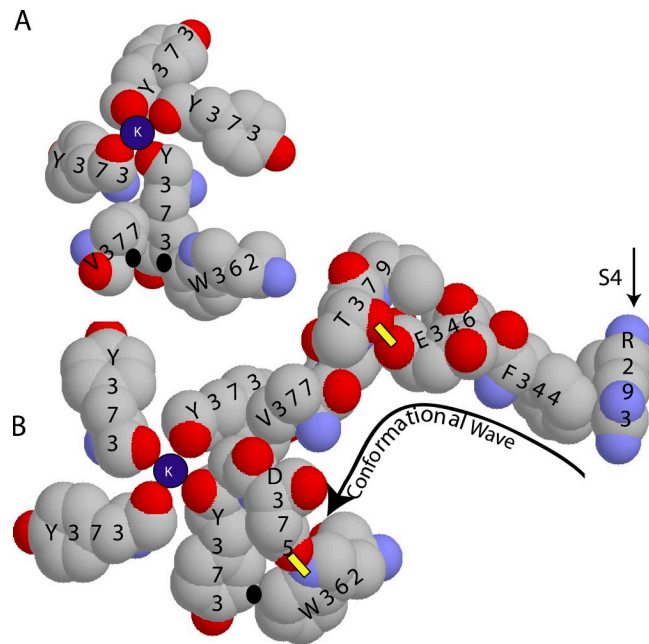


Figure 5. Structural model of C inactivation: the outer SF and surroundings from the 2R9R structure of the Long et al. (2007) model. (A) Residues V377 and W362 stabilize Y373 in the outer carbonyl ring of the SF. Points of close contact (<4 Å) are indicated by black dots. V377 is from an adjacent subunit. **(B)** Proposed conformational wave coupling S4 movement to the SF, beginning when outward S4 motion brings R293 in contact with F344. Yellow bars indicate important hydrogen bonds. Breaking the bond between D375 and W362 destabilizes Y373, which rotates away from the pore axis, reducing the affinity of the outer filter site for K^+ . The mutation W362F (W434F in Shaker) also eliminates this hydrogen bond and permanently C-inactivates the channel (Perozo et al., 1993).

Lowering the external K^+ concentration promotes C-type inactivation (Pardo et al., 1992; López-Barneo et al., 1993; Baukrowitz and Yellen, 1995) by lowering the probability of K^+ occupation, thus destabilizing the outer carbonyl ring. Finally, in the presence of high Ca^{2+} or La^{3+} , C inactivation occurs even at the resting potential; these multivalent ions gather at the outer mouth of the K channel when V_m is negative, producing a strong block of inward I_K . Because of strong hydration, Ca^{2+} and La^{3+} cannot enter the outer site of the filter, but they approach closely enough that their high charge (Ca^{2+} , La^{3+}) electrostatically pushes K^+ from the outer carbonyl ring, destabilizing the ring (Hoshi and Armstrong, 2013). Complete removal of K^+ inside and out totally removes K channel function, which slowly reverses upon restoration of K^+ (Gómez-Lagunas, 1997).

Merging structural data with physiology

Na channels are almost certainly derived from K channels, which are vital to the functioning of mitochondria and for osmotic stabilization of bacterial and eukaryotic cells (Armstrong, 2015). Fortunately, MacKinnon and colleagues have given us an excellent structural descrip-

tion of an open K channel (Long et al., 2005a,b, 2007), which is also helpful in understanding the Na channel. Known K channels have four identical domains, each composed of six transmembrane segments, with voltage dependence contributed by the charged S4 transmembrane segment (Sigworth, 1994; Larsson et al., 1996; Bezanilla, 2000). Similarly, bacterial Na channels have four identical domains (Ren et al., 2001; Koishi et al., 2004), suggesting their heritage from K channels. Unfortunately for present purposes, they lack the type of inactivation seen in Na channels from higher animals, e.g., squid and humans, in which the domains are differentiated. The differentiated S4 segments of higher animal Na channels vary in the number of gating charges in their S4 segments, from four to eight (Trimmer et al., 1989).

Detailed information on the arrangement of the S4 transmembrane segment, which, with its charged arginine and lysine residues, provides the voltage sensitivity of ion channels, comes mainly from the highly detailed crystal structure of the K channel (Long et al., 2005b, 2007). K channels have four identical domains, each containing six transmembrane segments: S1 through S6. Simplifying slightly, the fourth transmembrane segment, S4, has a series of five positively charged residues in a row (called the gating charges); each charge is separated from the next by two intervening hydrophobic residues, where R is arginine and K is lysine.

S4:	R1	xx	R2	xx	R3	xx	R4	xx	K5
S2:	E _o		E _i						F

These S4 residues move relative to a “charge transfer center” (Q_gTC; Tao et al., 2010) consisting, in the simplest case, of two negatively charged glutamate residues, E_o and E_i, separated by nine, intervening, hydrophobic residues; of which, two are phenyl-alanines, all located on the S2 helix. The negative charges in the Q_gTC make it possible for positive gating charges on the S4 to cross the hydrophobic barrier imposed by the hydrophobic residues in one jump, from E_o to E_i or the reverse. The glutamates E_o and E_i define the electrical outside and inside of the membrane, and R1–R4 jump electrically from inside to outside, or the reverse, over the high-resistance barrier imposed by the hydrophobic residues. When V_m is pushed from rest (approximately –70 mV) toward 0 mV, these positive “gating” charges are impelled outward, forcing the S4 segment outward through the membrane and producing a measurable I_g. This movement of the S4 allows a rearrangement of the inner “gate” region of S6, the channel-lining segment; its inner end spreads apart to allow passage of K⁺ ions. The recently solved structures of bacterial Na channels (Payandeh et al., 2011; Zhang et al., 2012), of the mammalian, skeletal muscle Ca channel (Wu et al., 2015, 2016) and of an insect Nav channel (Shen et al., 2017)

reveal that this structure for the voltage sensor, involving a Q_gTC, is probably common to all voltage-gated cation channels.

In the mammalian Na channel, there are, again, four domains, but all are different in sequence and properties. All Na channels have several behaviors that must somehow be related to these four domains. The first is *activation*, i.e., the resting channels are stimulated to open by a positive change of V_m imposed, e.g., by a synapse, a mechanoreceptor, or an advancing action potential. This causes the S4 segments to move outward and allows the “activation gate” to open. The gate is known from biophysical evidence to be at the inner end of the channel. In normal functioning, the consequent influx of Na⁺ drives V_m positive, further enhancing S4 movement, and driving V_m up to the peak of the action potential. To complete the action potential, the Na channels inactivate, and the K channels open relatively slowly, producing an efflux of K⁺ and driving V_m back to rest. The involvement of the four identical domains in the opening and closing of a K channel is relatively clear. The involvement of the Na channel’s four quite different domains has perplexed electrophysiologists for almost 30 years. Specifically, they wondered which domains, each with six transmembrane segments, are involved in activation and inactivation of the channel and how this molecular machinery is arranged to prevent the Na channel from leaking when it recovers from inactivation, as the K channel does when recovering from C9⁺-induced inactivation. Finally, one must explain how Na channels can inactivate without opening (Bean, 1981).

Many papers have attempted to measure the contribution of each charged residue to channel behavior and to the total charge movement during activation of a channel. The evaluation of the contribution to total charge movement was enormously simplified by the definition of the Q_gTC in 2010: each residue contributes one electronic charge as it moves from E_i to E_o or the reverse. Perhaps the major remaining questions are (1) which domains are associated with activation and which with inactivation; and (2) what is the involvement of each of the ~15 gating charges in activation and inactivation?

Much of the Na channel literature recently is concerned with these questions. An early answer to question 1, given by Horn et al. (2000), is that *all* domains contribute to activation and that D4:S4 in addition is involved in inactivation (see also Chen et al., 1996; Kontis and Goldin, 1997; Kontis et al., 1997; Mitrovic et al., 1998). Cha et al. (1999) found that inactivation immobilizes the D4 of S3 and S4, as determined in experiments using fluorescent labels at the top of the S4 of all four domains. Other articles suggest that activation is the function of S1–S3, and S4 is solely involved in inactivation (Chanda and Bezanilla, 2002; Hanck and

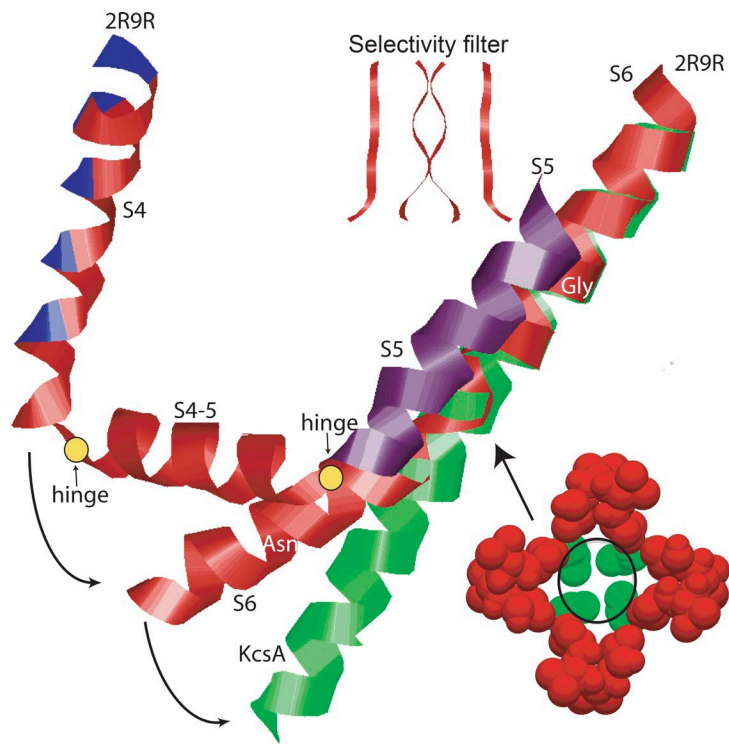


Figure 6. Ribbon diagrams. From a bacterial KcsA (green) and a Shaker-derived K channel (2R9R, red/purple). Structures were superimposed by aligning the SFs. The pore-lining TM2 segment of bacterial KcsA, which serves as a model for the closed channel, is almost straight. The outer half of the analogous pore-lining S6 segment of the 2R9R channel closely follows TM2 of KcsA near the outside and then bends away, part-way through the membrane, beginning near Gly marked on S6. Also shown for 2R9R are the S4 segment with positively charged residues in blue, the S4-5 linker (red), the S5 segment (purple, abbreviated), and two "hinges" (yellow). The curved arrows show guesses regarding the motions of S4, S4-5, and S6 as the channel closes. S4 moves downward, S4-5 pivots around a hinge at the junction of S4-5 with the S5 segment, and S4-S5 forces S6 to a position similar to the green KcsA helix. Cross sections of the channels, taken at the arrow, are shown at the lower right. Superimposed on the cross sections is a circle representing a hydrated K^+ ion, $\sim 8 \text{ \AA}$ in diameter. It is a good fit for the 2R9R channel, which is open. The KcsA channel has three hydrophobic seals (T107 is shown), which are too small for passage of a hydrated K^+ ion. In good agreement with this experimental setup, the cross section shows that a single one of the four S6s (or TM2s) in closed position is sufficient to stop I_K , which, at the gate, is a flux of hydrated K^+ .

Sheets, 2007; Capes et al., 2013). We give here our answer to this question: the S4s of all domains are involved in activation and the S4s of D3, and particularly D4, also govern inactivation.

Considerable mechanistic insight can be gained from the crystal structures of two K channels: the chimeric voltage-gated K channel, 2R9R (Long et al., 2007), and the bacterial KcsA channel (Doyle et al., 1998). Parts of these two structures are shown in Fig. 6. 2R9R serves as a model for the open state of a voltage-gated channel. This channel is clearly in the open state because the smallest diameter of its pore region, defined by the S6 segments, is $\sim 8 \text{ \AA}$, the diameter of a hydrated K^+ ion (Fig. 6, bottom right). At present, no structure is available for the closed state of 2R9R or any other voltage-gated K channel, forcing us to use the KcsA structure to approximate the closed state. This channel has three "hydrophobic seals," each with a diameter of $\sim 2 \text{ \AA}$, clearly too small for passage of a hydrated K^+ ion (Fig. 6, bottom right). In the main part of Fig. 6, the pore-lining TM2 transmembrane segment of KcsA is shown in green, a single, almost straight, transmembrane helix. The S4 of 2R9R is red, with positively charged residues in blue, whereas S4-S5 and S6 are red, and S5 is purple. S4 is the voltage-sensor effector of the 2R9R channel, and its multiple, positively charged residues move through the Q_g TC when V_m changes. S4 movement is approximated by the curved arrow. Downward movement of the S4 forces the S4-5 linker downward, rotating around a hinge at the intracellular end of S5. The

S5 (abbreviated for clarity) is fixed firmly in position by hydrophilic residues at its two ends. The downward motion of the S4 (in theory) presses the inner end of S6 into a closed position, similar to that of KcsA. Gly and Asn on the S6 segment mark the limits of a malleable region (containing PVP) that changes conformation during opening and closing.

Guided by this (theoretical) model from K channels, we present, in Fig. 7, a model of the more complicated Na channel, which has four distinct, rather than identical, domains. Fig. 7 shows only domains 2 and 4 (D2, D4) of a rat-brain Na channel. (We think D1 behavior is similar to D2.) The left-most diagram (Fig. 7 I) shows the closed state. NFE is the charge transfer center (Tao et al., 2010), found in the S2 segment of all four domains. Its outer site in D2 and D4 is a hydrophilic Asn (N), while in D1, it is Glu, and in D3, it is Asp. The inner site in all domains is a negatively charged Glu (E). These elements are separated by a hydrophobic sequence containing two phenylalanines. A residue in the inner site is, from the electrical viewpoint, inside, and it is electrically outside, when in the outer site. In D2 and D4, positive V_m works to drive an R (Arg) or K (Lys) from electrical inside (E) to the electrical outside (N), and negative V_m , from N to E. (Because almost all gating charges are outside at 0 mV, factors other than V_m are clearly involved in determining the exact in/out distribution of a gating charge at any voltage.) D2 has four charges that can move out or in through the Q_g TC, and D4 has seven (clear evidence of the exact

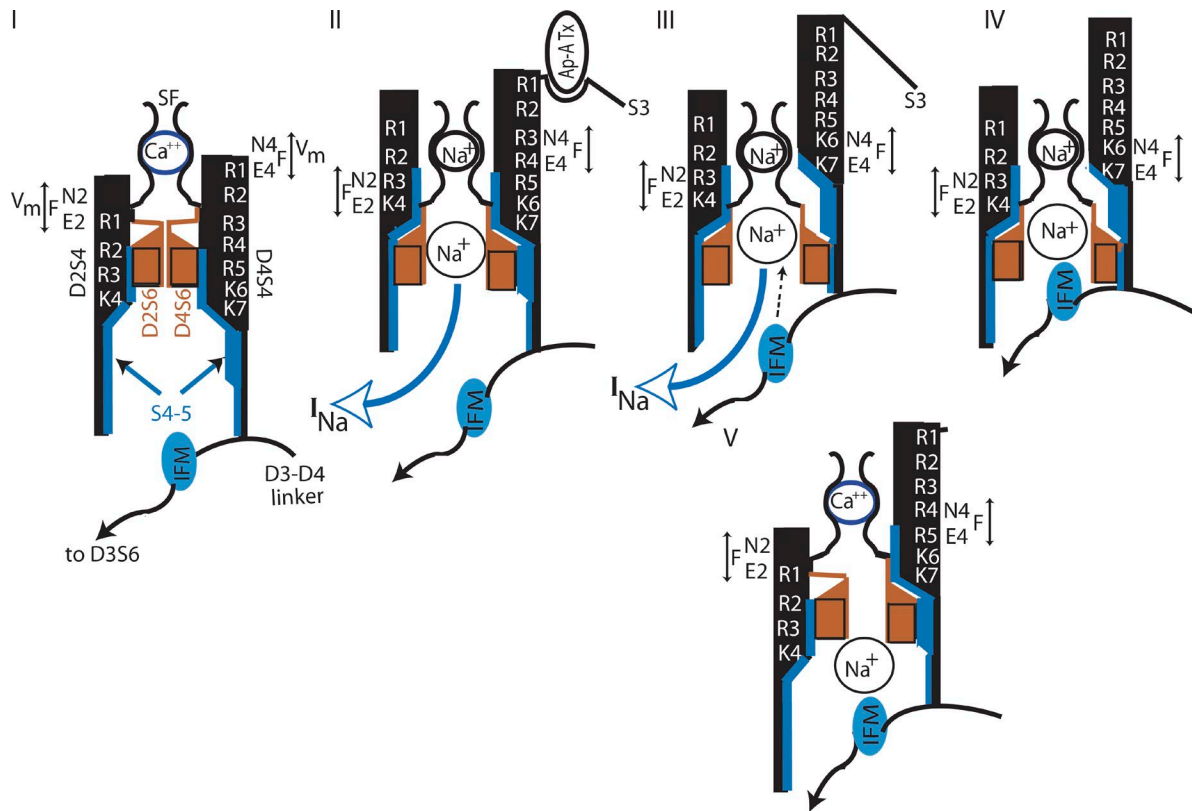


Figure 7. The states of a sodium channel. Closed (I), activated (II), ready to inactivate (III), inactivated (IV), and closed-inactivated (V). The S4 segments of D2 and D4 are in black, S4-5 linkers in blue, and S6 gate region in brown. The Q_gTC of D2 is E2 F N2, and for D4, it is E4 F N4. (I) The closed state. The S4s are in the full-inward position, with both D2:R1 and D4:R1 at E of their respective Q_gTC, pinching closed the S6 gate sections. The SF is occupied by a Ca²⁺ ion, pulled in by negative internal V_m . The D3-D4 linker and its IFM motif are held away from the channel's inner mouth by D4:S4. (II) D2:S4 and D4:S4 have moved outward, to the positions shown, allowing the S6 gates to open. The channel is conducting: a partially hydrated Na⁺ ion is in the SF, and a fully hydrated Na⁺ is in the gate region. Ap-A toxin is shown bound to the D4:S3-S4 linker, inhibiting further upward movement of D4:S4. (III) Ap-A toxin is either not present or has been displaced by prolonged depolarization. D4:S4 is fully activated, with K7 at E4. The inactivating particle is free to move upward (dashed arrow). (IV) The inactivating particle has moved into the inner mouth of the channel, stopping conduction. (V) On repolarization of the membrane, D2 (and D1, not depicted) have fully deactivated (R1 at E2) and closed the channel. R5 of D4 is at E4. Negative V_m has a) pulled a Ca²⁺ ion into the SF, and b) is forcing D4:S4 inward, which c) forces the inactivating particle out of the channel mouth, perhaps aided by the inward force on the Na⁺ ion, which is repelled by the Ca²⁺ ion in the SF. When the inactivating particle is dislodged, D4:S4 moves to fully deactivated position (R1 at E4), the S6 gate fully closes, and the channel has returned to condition I.

number of that move is not available: we make a reasonable guess). The SF is shown as occupied in the closed state by a tightly bound Ca²⁺ (for evidence, see Frankenreuser, 1957; Armstrong, 1999; Armstrong and Cota, 1999). Below the SF (in Fig. 7) is the vestibule and the gate region (brown), lined by the S6 segments. The inner surfaces of the S4 segments are lined in blue to represent the S4-5 linker. Finally, a segment of the D3-D4 linker, containing the IFM motif important in inactivation (West et al., 1992), is shown below the inner mouth of the channel.

Fig. 7 II shows the open state, achieved after three outward steps of the S4s. (We postulate that the motion of the S4s of the other two domains is similar.) Here, the inner S6 segments, no longer compressed by the S4-5 linkers, have sprung open, and Na⁺ ions move through

the channel; a partially dehydrated Na⁺ is shown in the SF, and a fully hydrated Na⁺ is shown in the gate region (brown).

The diagram in Fig. 7 (II and III) shows the effect of the Ap-A toxin, a site-3 toxin (Catterall, 1980, 1992). Site 3 is in the S3-S4 linker of D4 (Rogers et al., 1996; Benzinger et al., 1998). A channel bound by Ap-A toxin conducts I_{Na} normally but cannot inactivate (Hanck and Sheets, 1995). In Fig. 7 II, Ap-A toxin occupies a binding site in the S3-S4 linker of D4, stabilizing a (theoretical) kink that arrests movement of R4 to K7 through the Q_gTC, resulting in an ~30% reduction in total gating charge (Sheets and Hanck, 1995) and stopping the S4 motion before inactivation has occurred. We postulate that movement of R4 through K7 is responsible for the slow component of I_g shown in Fig. 3. The mutation D4

:R1/C has an effect similar to Ap-A, perhaps because a positive charge (e.g., as on the normal R1) is required to allow easy entry of the top of D4:S4 into the postulated kink in the S3–S4 linker. Because it arrests S4 motion with R4 in the Q_gTC, the R1/C mutation blocks several steps of S4 motion, and much more I_g than the one electron expected from neutralizing a single, positive charge (Sheets et al., 1999). In the absence of Ap-A, (or after Ap-A dissociates with prolonged depolarization from that postulated kink in the linker), S3–S4 stretches, as shown in Fig. 7 III, allowing completion of the outward motion of D4:S4.

Notice in Fig. 7 III that the upward movement of D4:S4 has made it possible for the D3–D4 linker, containing the IFM motif, to move upward, unhindered by D4:S4-5, and to approach the inner mouth of the channel. In Fig. 7 IV, the inactivation ball containing the IFM motif moves up to occlude the channel.

Consistent with this model, the mutation D4:R5H substantially slows inactivation near 0 mV (Kühn and Greeff, 1999). A possible explanation is that an uncharged histidine, substituted for R5, has a lower affinity for E4 and jumps more slowly into E4 after a depolarization to 0 mV. This slows inactivation without much affecting activation, which requires only S4 motion to place R4 in E4.

In Fig. 7 IV, the IFM motif stabilizes the inactivation ball by binding to the hydrophobic residues that line the channel. This occludes the channel sufficiently that the hydrated Na^+ shown in the gating region cannot pass through to the inside. We think that the KIFMK peptide, which, to some degree, mimics inactivation, has a similar arrangement: the positively charged lysine of the peptide takes the place of the hydrated Na^+ shown in the diagram, and IFM provides stable attachment to the hydrophobic lining of the channel. Finally, the lysine, at the inner end of the peptide, replaces the D3–D4 linker and keeps the inner end of the peptide in the internal medium. The overall result is that KIFMK is an “open channel blocker” of the Na channel (Eaholtz et al., 1994), quite analogous to C9⁺, the open channel blocker of the K channel or to *N*-methylstrychnine, an open channel blocker of the Na channel (Cahalan, 1978).

On repolarization, the channel’s S4 segments are driven inward, leading to the state shown in Fig. 7 V. Several things are happening: (a) D2:S4 (and D1:S4, not depicted) move fully down, and their S6 gates occlude the gate region (as noted in the discussion of Fig. 6, even a single S6 in the closed position is sufficient to effectively block I_{Na}); (b) drawn by negative V_m , Ca^{2+} moves into the SF (Frankenhaeuser, 1957; Armstrong, 1999; Armstrong and Cota, 1999), providing a strong repulsive force tending to displace the Na^+ and the D3–D4 linker from the gate region; and (c) the squeezing action by the S6 gate, in combination with repulsion

from the Ca^{2+} ion in the SF, helps force the hydrated Na^+ and the S3–S4 linker out of the channel, making it possible to fully close the S6 gate. This happens relatively slowly, accounting for the refractory period. The mutation D4:R4H (Kühn and Greeff, 1999) and D4:R4C (Groome et al., 2002) greatly slow recovery from inactivation. In terms of the diagram, when neutralized, this residue is not rapidly driven through the Q_gTC from N4 to E4 by negative V_m as would be arginine in this position. Thus, inactivation recovery is slowed.

With a small depolarization of long duration, it is possible to pass directly from the closed (Fig. 7 I) to the closed, inactivated (Fig. 7 V) state (Bean, 1981), perhaps because of the high affinity of K6 and K7 of D4 for E4 (cf., Tao et al., 2010).

A final word on the interesting article of Sheets et al. (2015). They examined the effect of mutations in the S6 of D3 and D4: N1462C and N1746C ($\text{Na}_v1.5$). Mutation of the latter residue, which is in the gate region of the D4:S6, virtually eliminates Na conductance, without altering charge movement. (Swartz and colleagues have performed similar mutations on K channels [Hackos et al., 2002].) We think this provides excellent evidence that S4:D4 is involved in both inactivation and activation gating (cf., Horn et al., 2000). We postulate (a) that the gating region of the S6s in all domains is unlocked by upward movement of the S4 and (b) that to open, the S6 of D4 must then undergo a further transition, which requires transfer of N1746, a highly hydrophilic Asn residue, to an aqueous environment. In the resting state, this step is inhibited by strong pressure on the S6 from the S4–S5 linker. With N1746C, transferring a Cys residue, rather than an Asn, to water is energetically less favorable by 6.8 kcal/mol (Engelman et al., 1986) or a factor of $\sim 8 \times 10^4$ at 25°C. Because all four S6s must be in gate-open position for the channel to conduct, g_{Na} is completely suppressed without altering gating charge movement by the N1746C mutation.

ACKNOWLEDGMENTS

The authors thank Toshi Hoshi and Carol Deutsch for helpful discussions during the preparation of this manuscript.

The authors declare no competing financial interests.
Olaf S. Andersen served as editor.

REFERENCES

- Agnew, W.S., A.C. Moore, S.R. Levinson, and M.A. Raftery. 1980. Identification of a large molecular weight peptide associated with a tetrodotoxin binding protein from the electroplax of *Electrophorus electricus*. *Biochem. Biophys. Res. Commun.* 92:860–866. [https://doi.org/10.1016/0006-291X\(80\)90782-2](https://doi.org/10.1016/0006-291X(80)90782-2)
- Aldrich, R.W., D.P. Corey, and C.F. Stevens. 1983. A reinterpretation of mammalian sodium channel gating based on single channel recording. *Nature*. 306:436–441. <https://doi.org/10.1038/306436a0>
- Armstrong, C.M. 1969. Inactivation of the potassium conductance and related phenomena caused by quaternary ammonium ion

injection in squid axons. *J. Gen. Physiol.* 54:553–575. <https://doi.org/10.1085/jgp.54.5.553>

Armstrong, C.M. 1971. Interaction of tetraethylammonium ion derivatives with the potassium channels of giant axons. *J. Gen. Physiol.* 58:413–437. <https://doi.org/10.1085/jgp.58.4.413>

Armstrong, C.M. 1981. Sodium channels and gating currents. *Physiol. Rev.* 61:644–683.

Armstrong, C.M. 1999. Distinguishing surface effects of calcium ion from pore-occupancy effects in Na^+ channels. *Proc. Natl. Acad. Sci. USA* 96:4158–4163. <https://doi.org/10.1073/pnas.96.7.4158>

Armstrong, C.M. 2007. Life among the axons. *Annu. Rev. Physiol.* 69:1–18. <https://doi.org/10.1146/annurev.physiol.69.120205.124448>

Armstrong, C.M. 2015. Packaging life: the origin of ion-selective channels. *Biophys. J.* 109:173–177. <https://doi.org/10.1016/j.bpj.2015.06.012>

Armstrong, C.M., and F. Bezanilla. 1973. Currents related to movement of the gating particles of the sodium channels. *Nature*. 242:459–461. <https://doi.org/10.1038/242459a0>

Armstrong, C.M., and F. Bezanilla. 1977. Inactivation of the sodium channel. II. Gating current experiments. *J. Gen. Physiol.* 70:567–590. <https://doi.org/10.1085/jgp.70.5.567>

Armstrong, C.M., and G. Cota. 1999. Calcium block of Na^+ channels and its effect on closing rate. *Proc. Natl. Acad. Sci. USA* 96:4154–4157. <https://doi.org/10.1073/pnas.96.7.4154>

Armstrong, C.M., F. Bezanilla, and E. Rojas. 1973. Destruction of sodium conductance inactivation in squid axons perfused with pronase. *J. Gen. Physiol.* 62:375–391. <https://doi.org/10.1085/jgp.62.4.375>

Baukowitz, T., and G. Yellen. 1995. Modulation of K^+ current by frequency and external $[\text{K}^+]$: a tale of two inactivation mechanisms. *Neuron*. 15:951–960. [https://doi.org/10.1016/0896-6273\(95\)90185-X](https://doi.org/10.1016/0896-6273(95)90185-X)

Baumann, A., I. Krah-Jentgens, R. Müller, F. Müller-Holtkamp, R. Seidel, N. Kecskemethy, J. Casal, A. Ferrus, and O. Pongs. 1987. Molecular organization of the maternal effect region of the Shaker complex of *Drosophila*: Characterization of an I(A) channel transcript with homology to vertebrate Na channel. *EMBO J.* 6:3419–3429.

Bean, B.P. 1981. Sodium channel inactivation in the crayfish giant axon. Must channels open before inactivating? *Biophys. J.* 35:595–614. [https://doi.org/10.1016/S0006-3495\(81\)84815-1](https://doi.org/10.1016/S0006-3495(81)84815-1)

Benzinger, G.R., J.W. Kyle, K.M. Blumenthal, and D.A. Hanck. 1998. A specific interaction between the cardiac sodium channel and site-3 toxin anthopleurin B. *J. Biol. Chem.* 273:80–84. <https://doi.org/10.1074/jbc.273.1.80>

Bezanilla, F. 2000. The voltage sensor in voltage-dependent ion channels. *Physiol. Rev.* 80:555–592.

Bezanilla, F., and C.M. Armstrong. 1977. Inactivation of the sodium channel. I. Sodium current experiments. *J. Gen. Physiol.* 70:549–566. <https://doi.org/10.1085/jgp.70.5.549>

Cahalan, M.D. 1978. Local anesthetic block of sodium channels in normal and pronase-treated squid giant axons. *Biophys. J.* 23:285–311. [https://doi.org/10.1016/S0006-3495\(78\)85449-6](https://doi.org/10.1016/S0006-3495(78)85449-6)

Capes, D.L., M.P. Goldschen-Ohm, M. Arcisio-Miranda, F. Bezanilla, and B. Chanda. 2013. Domain IV voltage-sensor movement is both sufficient and rate limiting for fast inactivation in sodium channels. *J. Gen. Physiol.* 142:101–112. <https://doi.org/10.1085/jgp.201310998>

Catterall, W.A. 1980. Neurotoxins that act on voltage-sensitive sodium channels in excitable membranes. *Annu. Rev. Pharmacol. Toxicol.* 20:15–43. <https://doi.org/10.1146/annurev.pa.20.040180.000311>

Catterall, W.A. 1992. Cellular and molecular biology of voltage-gated sodium channels. *Physiol. Rev.* 72(Suppl 4):S15–S48.

Cha, A., P.C. Ruben, A.L. George Jr., E. Fujimoto, and F. Bezanilla. 1999. Voltage sensors in domains III and IV, but not I and II, are immobilized by Na^+ channel fast inactivation. *Neuron*. 22:73–87. [https://doi.org/10.1016/S0896-6273\(00\)80680-7](https://doi.org/10.1016/S0896-6273(00)80680-7)

Chanda, B., and F. Bezanilla. 2002. Tracking voltage-dependent conformational changes in skeletal muscle sodium channel during activation. *J. Gen. Physiol.* 120:629–645. <https://doi.org/10.1085/jgp.20028679>

Chen, L.Q., V. Santarelli, R. Horn, and R.G. Kallen. 1996. A unique role for the S4 segment of domain 4 in the inactivation of sodium channels. *J. Gen. Physiol.* 108:549–556. <https://doi.org/10.1085/jgp.108.6.549>

Doyle, D.A., J. Morais Cabral, R.A. Pfuetzner, A. Kuo, J.M. Gulbis, S.L. Cohen, B.T. Chait, and R. MacKinnon. 1998. The structure of the potassium channel: molecular basis of K^+ conduction and selectivity. *Science*. 280:69–77. <https://doi.org/10.1126/science.280.5360.69>

Eaholtz, G., T. Scheuer, and W.A. Catterall. 1994. Restoration of inactivation and block of open sodium channels by an inactivation gate peptide. *Neuron*. 12:1041–1048. [https://doi.org/10.1016/0896-6273\(94\)90312-3](https://doi.org/10.1016/0896-6273(94)90312-3)

Engelman, D.M., T.A. Steitz, and A. Goldman. 1986. Identifying nonpolar transbilayer helices in amino acid sequences of membrane proteins. *Annu. Rev. Biophys. Biophys. Chem.* 15:321–353. <https://doi.org/10.1146/annurev.bb.15.060186.001541>

Fitzhugh, R. 1965. A kinetic model of the conductance changes in nerve membrane. *J. Cell. Comp. Physiol.* 66(S2):111–117. <https://doi.org/10.1002/jcp.1030660518>

Frankenhaeuser, B. 1957. The effect of calcium on the myelinated nerve fibre. *J. Physiol.* 137:245–260. <https://doi.org/10.1113/jphysiol.1957.sp005809>

Gómez-Lagunas, F. 1997. Shaker B K^+ conductance in Na^+ solutions lacking K^+ ions: A remarkably stable non-conducting state produced by membrane depolarizations. *J. Physiol.* 499:3–15.

Groome, J., E. Fujimoto, L. Walter, and P. Ruben. 2002. Outer and central charged residues in DIVS4 of skeletal muscle sodium channels have differing roles in deactivation. *Biophys. J.* 82:1293–1307. [https://doi.org/10.1016/S0006-3495\(02\)75485-4](https://doi.org/10.1016/S0006-3495(02)75485-4)

Hackos, D.H., T.H. Chang, and K.J. Swartz. 2002. Scanning the intracellular S6 activation gate in the Shaker K^+ channel. *J. Gen. Physiol.* 119:521–531. <https://doi.org/10.1085/jgp.20028569>

Hamil, O.P., A. Marty, E. Neher, B. Sakmann, and F.J. Sigworth. 1981. Improved patch-clamp techniques for high-resolution current recording from cells and cell-free membrane patches. *Pflügers Arch.* 391:85–100. <https://doi.org/10.1007/BF00656997>

Hanck, D.A., and M.F. Sheets. 1995. Modification of inactivation in cardiac sodium channels: ionic current studies with Anthopleurin-A toxin. *J. Gen. Physiol.* 106:601–616. <https://doi.org/10.1085/jgp.106.4.601>

Hanck, D.A., and M.F. Sheets. 2007. Site-3 toxins and cardiac sodium channels. *Toxicon*. 49:181–193. <https://doi.org/10.1016/j.toxicon.2006.09.017>

Hille, B. 1971. The permeability of the sodium channel to organic cations in myelinated nerve. *J. Gen. Physiol.* 58:599–619. <https://doi.org/10.1085/jgp.58.6.599>

Hille, B. 1975. The receptor for tetrodotoxin and saxitoxin. A structural hypothesis. *Biophys. J.* 15:615–619. [https://doi.org/10.1016/S0006-3495\(75\)85842-5](https://doi.org/10.1016/S0006-3495(75)85842-5)

Hodgkin, A.L., and A.F. Huxley. 1952a. Currents carried by sodium and potassium ions through the membrane of the giant axon of *Loligo*. *J. Physiol.* 116:449–472. <https://doi.org/10.1113/jphysiol.1952.sp004717>

Hodgkin, A.L., and A.F. Huxley. 1952b. The components of membrane conductance in the giant axon of *Loligo*. *J. Physiol.* 116:473–496. <https://doi.org/10.1113/jphysiol.1952.sp004718>

Hodgkin, A.L., and A.F. Huxley. 1952c. The dual effect of membrane potential on sodium conductance in the giant axon of *Loilgo*. *J. Physiol.* 116:497–506. <https://doi.org/10.1113/jphysiol.1952.sp004719>

Hodgkin, A.L., and A.F. Huxley. 1952d. A quantitative description of membrane current and its application to conduction and excitation in nerve. *J. Physiol.* 117:500–544. <https://doi.org/10.1113/jphysiol.1952.sp004764>

Horn, R., S. Ding, and H.J. Gruber. 2000. Immobilizing the moving parts of voltage-gated ion channels. *J. Gen. Physiol.* 116:461–476. <https://doi.org/10.1085/jgp.116.3.461>

Hoshi, T., and C.M. Armstrong. 2013. C-type inactivation of voltage-gated K⁺ channels: Pore constriction or dilation? *J. Gen. Physiol.* 141:151–160. <https://doi.org/10.1085/jgp.201210888>

Hoshi, T., W.N. Zagotta, and R.W. Aldrich. 1990. Biophysical and molecular mechanisms of *Shaker* potassium channel inactivation. *Science*. 250:533–538. <https://doi.org/10.1126/science.2122519>

Hoshi, T., W.N. Zagotta, and R.W. Aldrich. 1991. Two types of inactivation in Shaker K⁺ channels: effects of alterations in the carboxy-terminal region. *Neuron*. 7:547–556. [https://doi.org/10.1016/0896-6273\(91\)90367-9](https://doi.org/10.1016/0896-6273(91)90367-9)

Kamb, A., L.E. Iverson, and M.A. Tanouye. 1987. Molecular characterization of *Shaker*, a *Drosophila* gene that encodes a potassium channel. *Cell*. 50:405–413. [https://doi.org/10.1016/0092-8674\(87\)90494-6](https://doi.org/10.1016/0092-8674(87)90494-6)

Koishi, R., H. Xu, D. Ren, B. Navarro, B.W. Spiller, Q. Shi, and D.E. Clapham. 2004. A superfamily of voltage-gated sodium channels in bacteria. *J. Biol. Chem.* 279:9532–9538. <https://doi.org/10.1074/jbc.M313100200>

Kontis, K.J., and A.L. Goldin. 1997. Sodium channel inactivation is altered by substitution of voltage sensor positive charges. *J. Gen. Physiol.* 110:403–413. <https://doi.org/10.1085/jgp.110.4.403>

Kontis, K.J., A. Rounaghi, and A.L. Goldin. 1997. Sodium channel activation gating is affected by substitutions of voltage sensor positive charges in all four domains. *J. Gen. Physiol.* 110:391–401. <https://doi.org/10.1085/jgp.110.4.391>

Kühn, F.J., and N.G. Greeff. 1999. Movement of voltage sensor S4 in domain 4 is tightly coupled to sodium channel fast inactivation and gating charge immobilization. *J. Gen. Physiol.* 114:167–183. <https://doi.org/10.1085/jgp.114.2.167>

Larsson, H.P., O.S. Baker, D.S. Dhillon, and E.Y. Isacoff. 1996. Transmembrane movement of the Shaker K⁺ channel S4. *Neuron*. 16:387–397. [https://doi.org/10.1016/S0896-6273\(00\)80056-2](https://doi.org/10.1016/S0896-6273(00)80056-2)

Long, S.B., E.B. Campbell, and R. Mackinnon. 2005a. Crystal structure of a mammalian voltage-dependent Shaker family K⁺ channel. *Science*. 309:897–903. <https://doi.org/10.1126/science.1116269>

Long, S.B., E.B. Campbell, and R. Mackinnon. 2005b. Voltage sensor of Kv1.2: structural basis of electromechanical coupling. *Science*. 309:903–908. <https://doi.org/10.1126/science.1116270>

Long, S.B., X. Tao, E.B. Campbell, and R. MacKinnon. 2007. Atomic structure of a voltage-dependent K⁺ channel in a lipid membrane-like environment. *Nature*. 450:376–382. <https://doi.org/10.1038/nature06265>

López-Barneo, J., T. Hoshi, S.H. Heinemann, and R.W. Aldrich. 1993. Effects of external cations and mutations in the pore region on C-type inactivation of Shaker potassium channels. *Receptors Channels*. 1:61–71.

Mitrovic, N., A.L. George Jr., and R. Horn. 1998. Independent versus coupled inactivation in sodium channels. Role of the domain 2 S4 segment. *J. Gen. Physiol.* 111:451–462. <https://doi.org/10.1085/jgp.111.3.451>

Neher, E., and B. Sakmann. 1976. Single-channel currents recorded from membrane of denervated frog muscle fibres. *Nature*. 260:799–802. <https://doi.org/10.1038/260799a0>

Neher, E., B. Sakmann, and J.H. Steinbach. 1978. The extracellular patch clamp: a method for resolving currents through individual open channels in biological membranes. *Pflugers Arch.* 375:219–228. <https://doi.org/10.1007/BF00584247>

Noda, M., S. Shimizu, T. Tanabe, T. Takai, T. Kayano, T. Ikeda, H. Takahashi, H. Nakayama, Y. Kanaoka, N. Minamino, et al. 1984. Primary structure of *Electrophorus electricus* sodium channel deduced from cDNA sequence. *Nature*. 312:121–127. <https://doi.org/10.1038/312121a0>

Papazian, D.M., T.L. Schwarz, B.L. Tempel, Y.N. Jan, and L.Y. Jan. 1987. Cloning of genomic and complementary DNA from Shaker, a putative potassium channel gene from *Drosophila*. *Science*. 237:749–753. <https://doi.org/10.1126/science.2441470>

Pardo, L.A., S.H. Heinemann, H. Terlau, U. Ludewig, C. Lorra, O. Pongs, and W. Stühmer. 1992. Extracellular K⁺ specifically modulates a rat brain K⁺ channel. *Proc. Natl. Acad. Sci. USA*. 89:2466–2470. <https://doi.org/10.1073/pnas.89.6.2466>

Payandeh, J., T. Scheuer, N. Zheng, and W.A. Catterall. 2011. The crystal structure of a voltage-gated sodium channel. *Nature*. 475:353–358. <https://doi.org/10.1038/nature10238>

Perozo, E., D.M. Papazian, E. Stefani, and F. Bezanilla. 1992. Gating currents in Shaker K⁺ channels. Implications for activation and inactivation models. *Biophys. J.* 62:160–168. [https://doi.org/10.1016/S0006-3495\(92\)81802-7](https://doi.org/10.1016/S0006-3495(92)81802-7)

Perozo, E., R. MacKinnon, F. Bezanilla, and E. Stefani. 1993. Gating currents from a nonconducting mutant reveal open-closed conformations in Shaker K⁺ channels. *Neuron*. 11:353–358. [https://doi.org/10.1016/0896-6273\(93\)90190-3](https://doi.org/10.1016/0896-6273(93)90190-3)

Ren, D., B. Navarro, H. Xu, L. Yue, Q. Shi, and D.E. Clapham. 2001. A prokaryotic voltage-gated sodium channel. *Science*. 294:2372–2375. <https://doi.org/10.1126/science.1065635>

Rogers, J.C., Y. Qu, T.N. Tanada, T. Scheuer, and W.A. Catterall. 1996. Molecular determinants of high affinity binding of alpha-scorpion toxin and sea anemone toxin in the S3-S4 extracellular loop in domain IV of the Na⁺ channel alpha subunit. *J. Biol. Chem.* 271:15950–15962. <https://doi.org/10.1074/jbc.271.27.15950>

Sheets, M.F., and D.A. Hanck. 1995. Voltage-dependent open-state inactivation of cardiac sodium channels: Gating current studies with Anthopleurin-A toxin. *J. Gen. Physiol.* 106:617–640. <https://doi.org/10.1085/jgp.106.4.617>

Sheets, M.F., J.W. Kyle, R.G. Kallen, and D.A. Hanck. 1999. The Na⁺ channel voltage sensor associated with inactivation is localized to the external charged residues of domain IV, S4. *Biophys. J.* 77:747–757. [https://doi.org/10.1016/S0006-3495\(99\)76929-8](https://doi.org/10.1016/S0006-3495(99)76929-8)

Sheets, M.F., H.A. Fozard, and D.A. Hanck. 2015. Important Role of Asparagines in Coupling the Pore and Votage-Sensor Domain in Voltage-Gated Sodium Channels. *Biophys. J.* 109:2277–2286. <https://doi.org/10.1016/j.bpj.2015.10.012>

Shen, H., Q. Zhou, X. Pan, Z. Li, J. Wu, and N. Yan. 2017. Structure of a eukaryotic voltage-gated sodium channel at near-atomic resolution. *Science*. 355:eaal4326. <https://doi.org/10.1126/science.aal4326>

Sigworth, F.J. 1994. Voltage gating of ion channels. *Q. Rev. Biophys.* 27:1–40. <https://doi.org/10.1017/S0033583500002894>

Stefani, E., L. Toro, E. Perozo, and F. Bezanilla. 1994. Gating of Shaker K⁺ channels: I. Ionic and gating currents. *Biophys. J.* 66:996–1010. [https://doi.org/10.1016/S0006-3495\(94\)80881-1](https://doi.org/10.1016/S0006-3495(94)80881-1)

Stühmer, W., F. Conti, H. Suzuki, X.D. Wang, M. Noda, N. Yahagi, H. Kubo, and S. Numa. 1989. Structural parts involved in activation and inactivation of the sodium channel. *Nature*. 339:597–603. <https://doi.org/10.1038/339597a0>

Tao, X., A. Lee, W. Limapichat, D.A. Dougherty, and R. MacKinnon. 2010. A gating charge transfer center in voltage sensors. *Science*. 328:67–73. <https://doi.org/10.1126/science.1185954>

Tempel, B.L., D.M. Papazian, T.L. Schwarz, Y.N. Jan, and L.Y. Jan. 1987. Sequence of a probable potassium channel component encoded at Shaker locus of *Drosophila*. *Science*. 237:770–775. <https://doi.org/10.1126/science.2441471>

Trimmer, J.S., S.S. Cooperman, S.A. Tomiko, J.Y. Zhou, S.M. Crean, M.B. Boyle, R.G. Kallen, Z.H. Sheng, R.L. Barchi, F.J. Sigworth, et al. 1989. Primary structure and functional expression of a mammalian skeletal muscle sodium channel. *Neuron*. 3:33–49. [https://doi.org/10.1016/0896-6273\(89\)90113-X](https://doi.org/10.1016/0896-6273(89)90113-X)

Vassilev, P.M., T. Scheuer, and W.A. Catterall. 1988. Identification of an intracellular peptide segment involved in sodium channel inactivation. *Science*. 241:1658–1661. <https://doi.org/10.1126/science.2458625>

West, J.W., D.E. Patton, T. Scheuer, Y. Wang, A.L. Goldin, and W.A. Catterall. 1992. A cluster of hydrophobic amino acid residues required for fast Na(+) -channel inactivation. *Proc. Natl. Acad. Sci. USA*. 89:10910–10914. <https://doi.org/10.1073/pnas.89.22.10910>

Wu, J., Z. Yan, Z. Li, C. Yan, S. Lu, M. Dong, and N. Yan. 2015. Structure of the voltage-gated calcium channel Cav1.1 complex. *Science*. 350:aad2395. <https://doi.org/10.1126/science.aad2395>

Wu, J., Z. Yan, Z. Li, X. Qian, S. Lu, M. Dong, Q. Zhou, and N. Yan. 2016. Structure of the voltage-gated calcium channel Ca_v1.1 at 3.6 Å resolution. *Nature*. 537:191–196. <https://doi.org/10.1038/nature19321>

Zagotta, W.N., and R.W. Aldrich. 1990. Voltage-dependent gating of Shaker A-type potassium channels in *Drosophila* muscle. *J. Gen. Physiol.* 95:29–60. <https://doi.org/10.1085/jgp.95.1.29>

Zagotta, W.N., T. Hoshi, and R.W. Aldrich. 1990. Restoration of inactivation in mutants of Shaker potassium channels by a peptide derived from ShB. *Science*. 250:568–571. <https://doi.org/10.1126/science.2122520>

Zhang, X., W. Ren, P. DeCaen, C. Yan, X. Tao, L. Tang, J. Wang, K. Hasegawa, T. Kumasaka, J. He, et al. 2012. Crystal structure of Na_vAP, an orthologue of the NaChBac voltage-gated sodium channel. *Nature*. 486:130–134.

Zhou, Y., J.H. Morais-Cabral, A. Kaufman, and R. MacKinnon. 2001. Chemistry of ion coordination and hydration revealed by a K⁺ channel-Fab complex at 2.0 Å resolution. *Nature*. 414:43–48. <https://doi.org/10.1038/35102009>